Stability limits for gap solitons in a Bose-Einstein condensate trapped in a time-modulated optical lattice

Thawatchai Mayteevarunyoo
Department of Telecommunication Engineering, Mahanakorn University of Technology, Bangkok 10530, Thailand

Boris A. Malomed
Department of Interdisciplinary Studies, School of Electrical Engineering, Faculty of Engineering, Tel Aviv University, Tel Aviv 69978, Israel

(Received 22 June 2006; published 21 September 2006)

We investigate stability of gap solitons (GSs) in the first two band gaps in the framework of the one-dimensional Gross-Pitaevskii equation, combining the repulsive nonlinearity and a moderately strong optical lattice (OL), which is subjected to "management," in the form of time-periodic modulation of its depth. The analysis is performed for parameters relevant to the experiment, characteristic values of the modulation frequency being $\omega \sim 2\pi \times 20$ Hz. First, we present several GS species in the two band gaps in the absence of the management. These include fundamental solitons and their bound states, as well as a *subfundamental* soliton in the second gap, featuring two peaks of opposite signs in a single well of the periodic potential. This soliton is always unstable, and quickly transforms into a fundamental GS, losing a considerable part of its norm. In the first band gap, (stable) bound states of two fundamental GSs are possible solely with opposite signs, if they are separated by an empty site. Under the periodic modulation of the OL depth, we identify stability regions for various GS species, in terms of ω and modulation amplitude, at fixed values of the soliton's norm, N. In either band gap, the GS species with smallest N has a largest stability area; in the first and second gaps, they are, respectively, the fundamental GS proper, or the one spontaneously generated from the subfundamental soliton. However, with the increase of N, the stability region of every species *expands* in the first gap, and *shrinks* in the second one. The outcome of the instability development is also different in the two band gaps: it is destruction of the GS in the first gap, and generation of extra side lobes by unstable GSs in the second one.

DOI: 10.1103/PhysRevA.74.033616 PACS number(s): 03.75.Lm, 05.45.Yv, 42.70.Qs

I. INTRODUCTION AND THE MODEL

An effective means for the control of dynamics of collective excitations in Bose-Einstein condensates (BECs) is provided by optical lattices (OLs), which are created as interference patterns by counterpropagating laser beams illuminating the condensate [1]. The spatially periodic distribution of the light intensity in the OL induces a periodic potential acting on atoms in the boson gas (atoms are attracted to or repelled from intensity maxima if the light building the OL is, respectively, red- or blue-detuned relative to the frequency of the internal dipole transition in the atom). The OLs are especially efficient in supporting matter-wave solitons. In particular, it has been predicted that two-dimensional (2D) [2–6] and 3D [2,5] OLs can stabilize solitons of the same dimension in BEC with attractive interactions between atoms (without the lattice, the corresponding soliton solutions exist too, but they are unstable against collapse). Moreover, it has been demonstrated that low-dimensional OLs, i.e., 1D and 2D lattice in the 2D [5,6] or 3D [5–7] case, respectively, can also stabilize fully localized multidimensional solitons, simultaneously giving them the freedom to move in the unrestricted direction [6]. A related result is the demonstration of the stability of 2D [8] and 3D [9] solitons in models with a cylindrical OL, which can be induced by a diffraction-free Bessel beam (see Ref. [8], and references therein).

If interactions between atoms in the BEC are repulsive (which is the most common case [10]), solitons cannot exist in the free space, but it was predicted that they could be supported, in the form of *gap solitons* (GSs), by periodic OL potentials, in 1D [11] and multidimensional [12] cases alike (a counterpart of this mean-field effect at the level of individual atoms is formation of a coherent state of two repulsively interacting atoms trapped in one well of the OL potential [13]). Creation of a GS in ^{87}Rb condensate in a quasi-1D trap supplemented by a longitudinal OL was reported in Refs. [1,14]; the soliton was built of a few hundred atoms. In a subsequent experiment, extended confined states containing a larger number of atoms were discovered in a stronger OL [15]; an explanation to this observation was proposed in Ref. [16], which, essentially, treated the extended state as a segment of a nonlinear Bloch wave, bounded by two fronts (domain walls) which are sustained by the strong OL (a similar OL-sustained border between filled and empty domains was predicted in BEC with self-attraction in Ref. [17]). In addition to the fundamental GSs, stable vortical solitons have also been predicted in the 2D repulsive BECs trapped in the square-shaped OL [5,18,19]. It is also relevant to mention that *radial gap solitons* can be predicted in the 2D repulsive condensate trapped in an axisymmetric potential which is a periodic function of the radial coordinate [20].

Another effective tool for testing and steering BEC dynamics is the use of periodic time modulation of various parameters affecting behavior of the condensate. These methods belong to the general class of *management* techniques, originally developed in nonlinear optics and then applied to BEC [21]. Among them are periodic time modula-

tion of the strength of the magnetic (parabolic-potential) trap confining a self-repulsive [22] or attractive [23] condensate, which gives rise to various parametric resonances in the BEC dynamics, and periodic time modulation of the nonlinearity coefficient (i.e., the scattering length of atomic collisions) via the Feshbach resonance in ac magnetic fields. The latter management mode was predicted to stabilize 2D solitons in free space [24] and 3D solitons in the presence of a quasi-1D OL potential [25]. In the 1D setting, the technique of the *Feshbach-resonance management* gives rise to dynamical states of a condensate trapped in the parabolic potential, such as breathers oscillating between Thomas-Fermi and quasisoliton configurations, and stable two-soliton states [26]. An effect predicted as a result of the interplay between the OL in two or one dimension and the periodic low-frequency modulation of the nonlinearity coefficient is the emergence of robust *alternate solitons*, whose shape adiabatically oscillates between those of the GS and ordinary soliton [27].

Various results outlined above suggest, as a natural extension of the study of the management techniques for BEC, to consider effects of periodic time modulation of the OL strength on the stability of GSs in self-repulsive condensates, which is the subject of the present work. In the experiment, the modulation can be easily realized by periodic attenuation of the intensity of the laser beams illuminating the condensate. As GSs cannot exist without the OL, it is quite interesting to explore the limits of their robustness against periodic variations of the amplitude of the lattice which supports them. It is relevant to note that gradual variation of the OL depth in time was already used in the experiment, with the objective to probe the linear band-gap spectrum induced by the lattice (in particular, to transfer atomic populations between different bands) [28]. Exploration of effects caused by the periodic variation of the lattice depth may lead to predictions for experiments aiming to test dynamical properties of condensates in the fully nonlinear regime.

In this paper, we focus on the GS stability limits in the 1D geometry (i.e., in "cigar-shaped" traps; the 2D situation will be considered separately). As is well known, the BEC dynamics in this case obeys the accordingly reduced (transversely averaged) Gross-Pitaevskii equation (GPE) [1,10,29]. In the normalized form, the equation is

$$i\frac{\partial u}{\partial t} = -\frac{1}{2}\frac{\partial^2 u}{\partial x^2} + |u|^2 u - V_0 \cos(2x)u. \tag{1}$$

Here $t \equiv T(\pi^2\hbar/md^2)$ and $x \equiv \pi X/d$, where T and X are the time and longitudinal coordinate in physical units, m the atomic mass, and d the lattice period. Further, $u(x,t)$ is the accordingly normalized effectively one-dimensional mean-field wave function (generated by averaging the full three-dimensional GPE in the transverse plane [29]), the corresponding full three-dimensional wave function being

$$\Psi(X,R,T) = \sqrt{\pi/(2a_s d^2)}u(x,t)\exp[-i\omega_\perp T - (\omega_\perp m/2\hbar)R^2],$$

where $\omega_\perp$ and R are the transverse trapping frequency and radial coordinate, and a_s the s-wave scattering length, all taken in physical units (in the underlying three-dimensional GPE, the coefficient in front of the nonlinear term is $4\pi\hbar^2 a_s$ [10]). In this setting, the lattice strength is represented by $V_0 = E_0/E_{\rm rec}$, where $E_{\rm rec} = (\pi\hbar)^2/(md^2)$ is the lattice recoil energy, and E_0 is the depth of the periodic potential, in physical units. In experiments with the ^{87}Rb condensate (which has $m = 1.4 \times 10^{-25}$ kg and $a_s = 5.77$ nm) [1], the lattice period varies between 0.4 and 1.6 μm, the corresponding normalized lattice depth being $V_0 \lesssim 20$. In this paper, we report results for $V_0 = 5$; comparison with other physically relevant values of V_0 shows that this case adequately represents the generic situation.

The main integral characteristic of the BEC is the norm, $N = \int_{-\infty}^{+\infty} |u(x)|^2 dx$, which is proportional to the number of trapped atoms. Together with the Hamiltonian,

$$H = \int_{-\infty}^{+\infty} \left[\frac{1}{2}|u_x|^2 + \frac{1}{2}|u|^4 - V_0 \cos(2x)|u|^2 \right] dx,$$

N is a dynamical invariant of Eq. (1).

Equation (1), being the nonlinear Schrödinger equation with a periodic external potential, is definitely nonintegrable, as well as Eq. (2) with the time-modulated potential [30] (see below), hence the term "soliton" is used in this work in a loose sense, as a synonym of a robust solitary pulse in a conservative model. We also note that, being interested in GSs whose size is essentially smaller than the effective longitudinal length of the trap, we do not add a parabolic trapping potential to Eq. (1).

To include the periodic time modulation of the OL depth at frequency ω, we replace Eq. (1) by the following one,

$$i\frac{\partial u}{\partial t} = -\frac{1}{2}\frac{\partial^2 u}{\partial x^2} + |u|^2 u - V_0\left[1 + \frac{\varepsilon}{2}\cos(\omega t)\right]\cos(2x)u, \tag{2}$$

where the modulation amplitude takes values $0 \leqslant \varepsilon < 2$ (obviously, the intensity modulation cannot change the sign of the OL potential, although the sign may be changed by translation of the OL, which amounts to a simple substitution, $x \to x \pm \pi/2$, and may be implemented through a change of the relative phase between the two laser beams, cf. techniques used to create moving OLs [31,32]). It is relevant to mention that a discrete limit of the GPE with a very strong OL, i.e., the discrete nonlinear Schrödinger equation (DNLSE), with periodic time modulation of the intersite coupling, which corresponds to the lattice management in Eq. (2), was introduced in Ref. [33]. The subject of that work was the modulational instability of a uniform state in the periodically "managed" DNLSE against parametric perturbations.

The paper is structured as follows. In Sec. II, we use Eq. (1) to describe several families of stable GSs supported by the static OL in its first and second finite band gaps. The families include both fundamental, *subfundamental* (whose meaning is explained below), and higher-order solitons (bound complexes). This set of solutions actually provides for a rather comprehensive (although not exhaustive) description of practically relevant GS families in the first two band gaps in the 1D model. Except for the subfundamental solitons and complexes which include them, all other GS species are found to be stable. Systematic results concerning stability limits of the GSs of these types in the time-modulated lattice, collected by means of massive direct

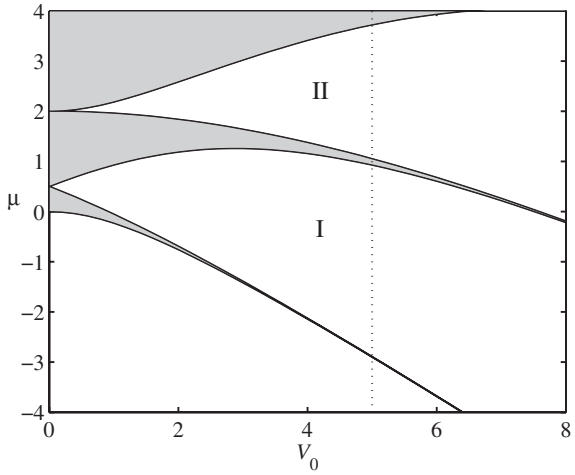

FIG. 1. The band-gap diagram for the linear version of Eq. (3). Band areas are shaded; numbered regions, I and II, are two lowest finite band gaps where gap solitons will be considered (the unshaded area below band gap I is the semi-infinite gap, where the Gross-Pitaevskii equation with the repulsive nonlinearity does not give rise to solitons). The dotted vertical line shows the particular value, $V_0=5$, for which typical results are presented below.

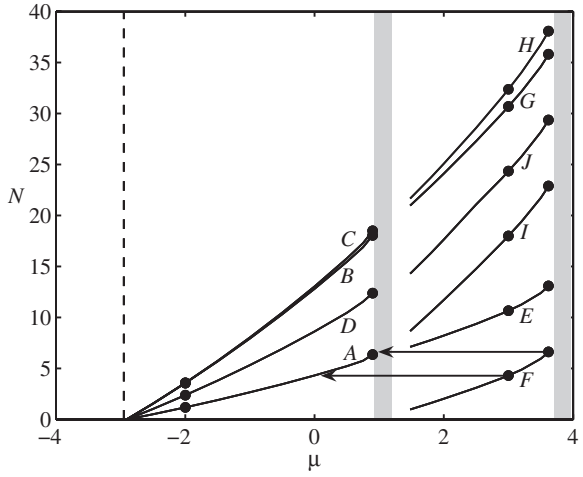

FIG. 2. Lowest-order families of gap solitons, shown in terms of the $N(\mu)$ dependence. Shapes of the gap solitons corresponding to the marked points are displayed in Figs. 3 and 4, for the first and second band gaps, respectively. The arrows originating from the marked points belonging to branch F of the *subfundamental* solitons in the second gap (see definition in the text) indicate that instability quickly rearranges them, with conspicuous loss of the norm, into fundamental solitons of type *A*, belonging to the *first* band gap.

simulations of Eq. (2), are reported in Sec. III. The results are summarized in the form of sets of stability borders in the (ε,ω) plane [recall ε and ω control the time modulation in Eq. (2)], at fixed values of the norm, N. Variation of the stability regions with N is investigated too; it is concluded that all stability regions in the first and second band gaps *expand* and *shrink*, respectively, with the increase of N. The paper is concluded by Sec. IV.

II. GAP-SOLITON FAMILIES IN THE STATIC LATTICE

Stationary GSs in the periodic potential are localized solutions to Eq. (1), $u(x,t)=\psi(x)\exp(-i\mu t)$, where real chemical potential μ and stationary wave function $\psi(x)$ obey the time-independent GPE,

$$\mu\psi = -\frac{1}{2}\frac{\partial^2\psi}{\partial x^2} + |\psi|^2\psi - V_0\cos(2x)\psi, \tag{3}$$

which, in the linear limit, goes over into the classical Mathieu equation. The band-gap spectrum of the latter equation is well known; for reference purposes, we display it in Fig. 1. To generate this figure, borders between bands and gaps were computed by using a numerical spectral method on interval $[0,2\pi]$. In the computations, we approximated the second derivative by a second-order spectral-differentiation matrix, and a diagonal matrix represented the periodic potential, $V_0\cos(2x)$.

Next, the full nonlinear stationary equation (3) was solved by means of Newton's method on a finite-difference grid, with an initial guess $\psi_0(x)=A_0\,\mathrm{sech}(ax)$ or $A_0\,\mathrm{sech}(ax)\sin(kx)$ (to generate even and odd solutions, respectively), where A_0, a, and k are free parameters (both initial *ansätze* were used in either band gap). The computations were run till a relative accuracy no worse than 10^{-6} was achieved, which usually required seven iterations of Newton's algorithm.

This way, known results for the GSs in the static OL with the repulsive nonlinearity were reproduced (and, in fact, some additional results for higher-order solitons were obtained too, see below). GSs were found in all finite band gaps explored. Several families of the lowest-order solitons in the first and second finite gaps, which will be considered below under the action of the periodic time modulation of the OL strength, are presented in Fig. 2, which shows the soliton's norm versus the chemical potential for each family. Typical shapes of the respective GSs are displayed in Figs. 3 and 4, which include two examples for each branch, one taken very close to the right edge of the respective band gap, and another one deeply inside the gap. The examples were chosen this way because, close to the edge, the shape changes conspicuously, developing a complex intrinsic structure, in comparison with a relatively simple shape of the GSs found deep inside the gaps. This complex structure may be realized as being similar to the Bloch functions of quasiperiodic linear states found on the other side of the band-gap border.

Fundamental solitons, which belong to branches *A* and *E* in the first and second band gaps in Fig. 2, are distinguished by the well-pronounced single peak (in particular, the fundamental GS in the first band gap, of type *A*, is trapped practically in a single potential well and is very similar to ordinary solitons in the one-dimensional GPE with the attractive nonlinearity and no OL). Some higher-order solitons may be clearly interpreted as bound states of two (branches *D*) or three (B,C,G,H) peaks corresponding to the fundamental solitons. It is noteworthy too that, alongside "densely packed" bound states (in particular, all three-peak ones), "rarefied" bound states are also found, such as the out-of-phase two-peak state *D* in the first gap. We stress that, in the

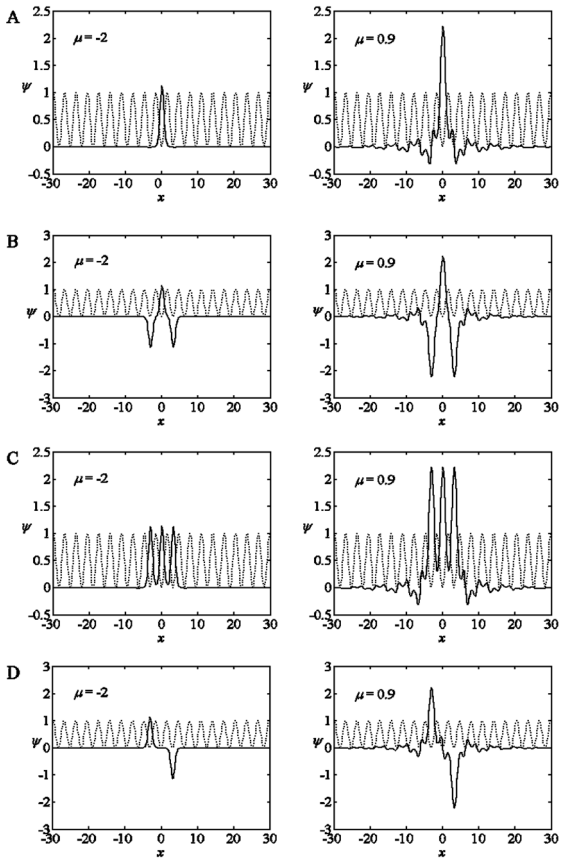

FIG. 3. Soliton profiles in the first band gap, which appertain to the labeled families in Fig. 2. Each branch is illustrated by two examples, the left one taken deep inside the gap, and the right one near the gap's edge. The dotted lines show the OL potential.

considered parameter region, two-peak bound states (in- or out-of-phase ones) without an empty site between them *have not* been found, probably because the interaction between two closely set peaks is too strong, and cannot be balanced by their pinning to the OL. It is also relevant to mention that a two-peak bound state like *D*, but with equal signs of the peaks, could not be found either.

The interpretation of states *D* and *B*, *C*, *G*, *H* as bound states of two and three fundamental solitons is well corroborated by the fact that their norms are close, respectively, to the double or triple norm of the fundamental soliton at the same value of μ, as seen in Fig. 2. On the other hand, we have also found several multipeak species that are *not* bound states of fundamental solitons, but have a clearly different nature. The most basic among such additional solitons is state *F* found in the second gap, which features two out-of-phase peaks, with a zero between them, squeezed into a *single* potential well. This localized solution may be considered as a soliton of a "dark-inside-bright" type; formally similar solitons (that are stable in a certain parameter region) were found in the GPE combining the OL potential or an external parabolic-potential trap and the attractive nonlinearity (on the contrary to the present model), in Ref. [34]. In that work, it was also demonstrated that, in the limit of a very strong OL, such solitons go over into known *twisted*

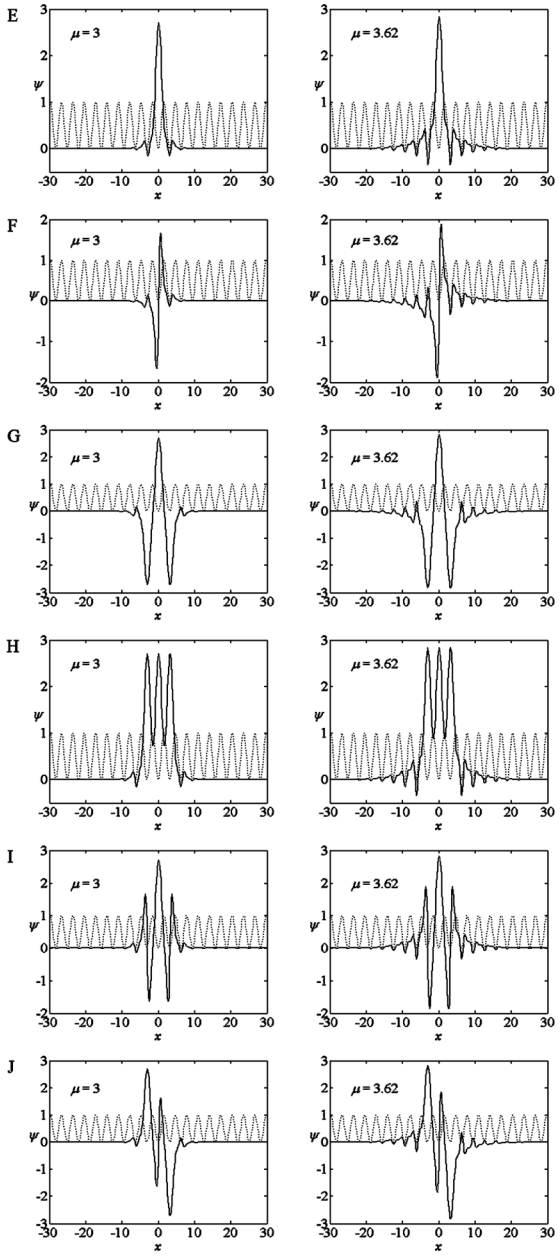

FIG. 4. The same as in Fig. 3, for the labeled gap-soliton branches belonging to the second band gap from Fig. 2.

localized modes [35] in the DNLSE model. However, the similarity of our type-*F* two-peak solitons to those reported in Ref. [34] is only formal, as the solitons found in Ref. [34] were, in fact, out-of-phase bound states of fundamental solitons, clearly located in two adjacent wells of the OL potential. State *F* in Fig. 4 is principally different, as seen from the fact that its norm is *much smaller* than that of the fundamental GS (of type *E*) found at the same value of μ, see Fig. 2; for this reason, we will call it a "subfundamental" GS. In fact, state *F* does not have any counterpart in the DNLSE model.

Direct simulations of the full GPE with the unmodulated OL potential, i.e., Eq. (3), demonstrate that the subfunda-

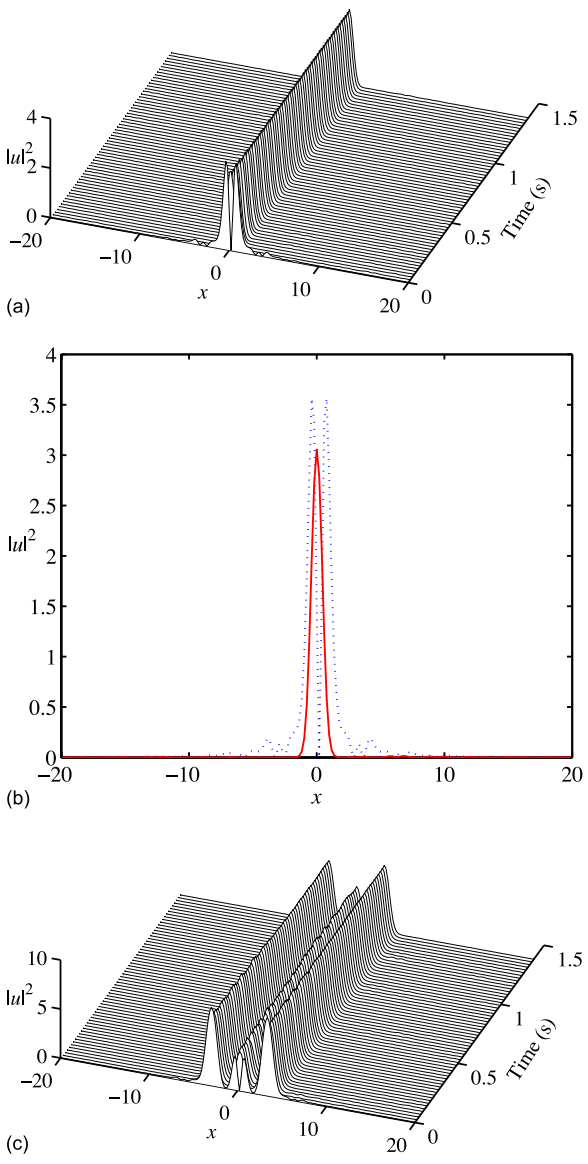

FIG. 5. (Color online) (a) Instability-induced spontaneous rearrangement of an the unstable *subfundamental* gap soliton, shown in panel *F* in the right column of Fig. 4 (μ=3.62, N=6.955), into a stable fundamental gap soliton, which keeps only 50% of the initial norm, and belongs to branch *A* in the first band gap; (b) comparison of the initial (dotted) and final (solid) shapes of the solitons in this case. (c) Similar spontaneous rearrangement of compound state *J*, which is made of a subfundamental soliton of type *F* and two fundamental solitons (the compound, corresponding to μ=3.62 and N=29.622, is shown in panel *J* in the right column of Fig. 4), into a stable bound state of three fundamental solitons. In this figure and all figures below, which display the temporal evolution of solitons, time is shown in typical physical units for the ^{87}Rb condensate.

mental solitons are *always unstable*, featuring, as shown in Figs. 5(a) and 5(b), rapid spontaneous rearrangement into a stable fundamental GS, with conspicuous loss of the norm, as illustrated by arrows in Fig. 2. Because of the loss, the stable fundamental solitons, into which the subfundamental ones relax, *always* fall into the first band gap. If soliton *F* is taken very close to the left edge of the second band gap (for instance, with initial norm N_0=7.318) it eventually loses (through emission of radiation) 50% of the norm, and the *F* soliton with N_0=4.416 keeps, in the end, only 51% of the norm. However, subfundamental solitons with a very small initial norm lose a small part of it; for instance, one with N_0=1.110 keeps 90% of the norm after the transformation into the fundamental soliton of type *A*.

In the second band gap, we have also found several species of higher-order solitons that may be considered as compounds including both fundamental and subfundamental GSs. In particular, species *I* (see Fig. 4) is a bound state of a fundamental GS (of type *E*), set at the center, and two subfundamental modes of type *F*; species *J* is built as a compound including two fundamental GSs and a subfundamental soliton between them. Accordingly, solitons of species *I* and *J* feature, respectively, five and four peaks per three wells of the periodic potential. These compound states feature the same instability of the subfundamental (type-*F*) constituent as in Fig. 5(a): it spontaneously transforms into a fundamental GS, losing a considerable part of its norm, while the regular constituents of the compound are not affected by this transition, see an example for the type-*J* state in Fig. 5(c).

The fundamental GSs (species *A* and *E* in Figs. 2–4), and their ordinary bound states (species *D* and *B*, *C*, *G*, *H*) were *all* found to be stable in direct simulations [typically, the simulations were run, by means of the split-step fast Fourier transform (FFT) method, with absorbers set at edges of the integration domain, up to t=10 000, which corresponds to an experimentally relevant time, $\simeq$1.4 s in the ^{87}Rb condensate]. It is interesting to compare findings concerning the stability of bound states in the present model, and a general conclusion for the stability of bound discrete solitons, drawn in the DNLSE model with the onsite self-focusing nonlinearity. In the latter context, it was concluded that a bound state of two fundamental solitons may only be stable if they have opposite signs [36]. Our model, however, relates to the DNLSE with self-defocusing nonlinearity, which, in the discrete system, can be transformed into its self-focusing counterpart by means of the known *staggering transformation*, $u_n \equiv (-1)^n \tilde{u}_n$, where n is the discrete coordinate on the lattice. Analysis of the stability of bound states of *staggered* DNLSE solitons (in the model with the self-attraction) yields results which are, roughly, inverse to the above-mentioned conclusion. In particular, a π-out-of-phase bound state of two staggered discrete solitons is never stable, while their in-phase bound state may be stable; an additional result is that the character of the stability reverses again if an empty site is inserted between two bound solitons [37]. These predictions agree with our observation that the loosely packed out-of-phase bound state of two fundamental GSs in the first band gap (species *D* in Figs. 2 and 3), and the densely packed in-phase states of three fundamental solitons (species *C* and *H*) are stable. Nevertheless, three-peak bound states with opposite signs of adjacent solitons (species *B* in Fig. 3 and *G* in Fig. 4) seem completely stable too. It may happen that instability of the latter state is extremely weak and remains invisible in the simulations, or the conclusions drawn in the DNLSE system cannot be transferred onto all types of bound states in the continuum GPE model.

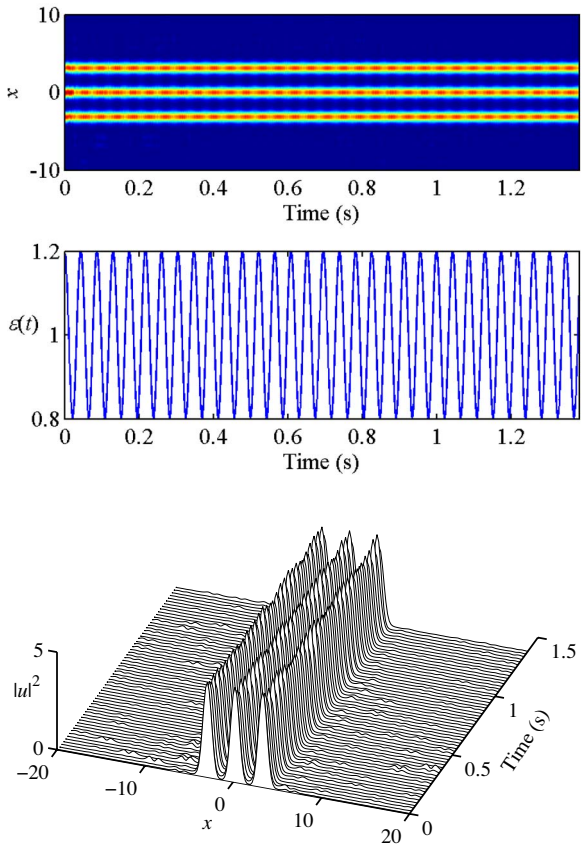

FIG. 6. (Color online) An example of the soliton of type B which remains stable under the action of the "lattice management," with $\varepsilon=0.4$ and $\omega=0.02$ (in physical units, this frequency, for which all other examples are displayed below, corresponds to $2\pi \times 20$ Hz). The initial profile of the soliton, which has norm $N=17.731$, is the same as in panel B in the right column of Fig. 3. Top and bottom panels display the spatiotemporal evolution of the density in terms of contour and three-dimensional plots.

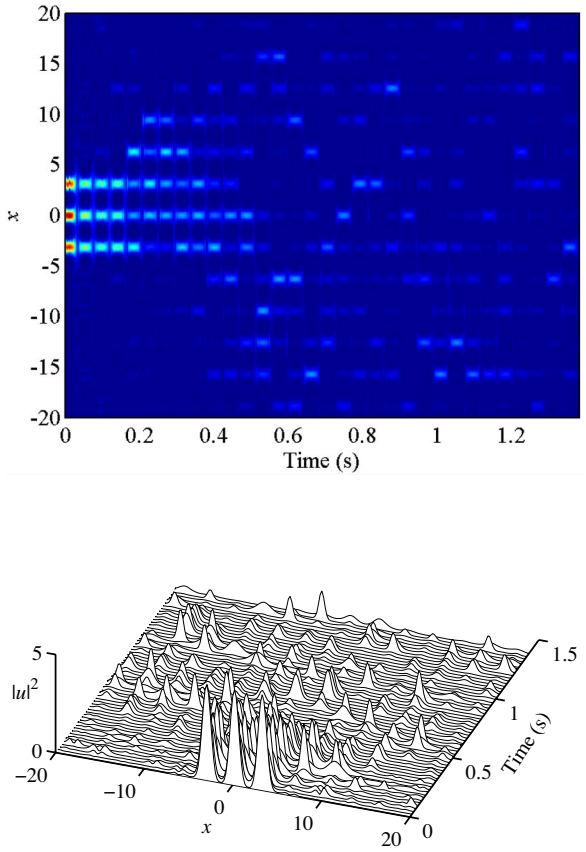

FIG. 7. (Color online) The same as in Fig. 6, but for an unstable soliton of type B, under the lattice management with $\varepsilon=1.8$ and $\omega=0.02$. The initial soliton is identical to that in Fig. 6.

III. STABILITY LIMITS OF GAP SOLITONS IN THE TIME-MODULATED LATTICE

A. Generic examples of stable and unstable solitons under the action of the lattice management

The stability or instability of solitons in Eq. (2) with the explicit time modulation was identified by means of sufficiently long direct simulations, with the initial condition taken as a stationary soliton of the corresponding equation without the "management," i.e., Eq. (3). Typical examples of solitons from the first band gap which turn out to be stable and unstable under the action of the lattice management are shown, respectively, in Figs. 6 and 7, for out-of-phase three-peak bound states of type B belonging to the first band gap. These examples and ones presented below are displayed for the modulation frequency $\omega=0.02$, which, in physical units, typically corresponds to $\simeq 2\pi \times 20$ Hz (in the case of the ^{87}Rb condensate).

In the first band gap, the only instability mode, as observed in all simulations under the lattice management, is direct destruction of the soliton, such as in Fig. 7. However, in the second band gap the instability develops in a different way (if the GS is unstable)—namely, by generating extra side lobes attached to the soliton, as seen in Fig. 8 for the fundamental GS (of type E). Additionally, Fig. 9 displays an example of multiple formation of side lobes, in the soliton of type G. The situations with the emergence of side lobes are categorized as unstable not only due to the conspicuous change in the soliton's shape, but also because of the loss of its norm: in truly stable cases, the norm loss is negligible, while in cases leading to the transformation of the GS into one with extra lobes, it loses $\sim 20\%$ of the norm.

A common feature of the picture of the instability onset and development in both band gaps, evident in the above examples (Figs. 7–9), is some (although not very strong) *spontaneous symmetry breaking* of unstable solitons. The feature may be explained by the fact that the instability amplifies very small random asymmetric numerical perturbations.

In the presence of the time modulation of the lattice, as well as in the model with the static OL, the subfundamental soliton in the second band gap—a free one (type F), or a constituent of a compound—rapidly transforms itself into a fundamental GS. Usually, the transformation happens earlier than the generation of the side lobes under the action of the lattice management (if the resulting fundamental or compound soliton is unstable under the lattice management). An

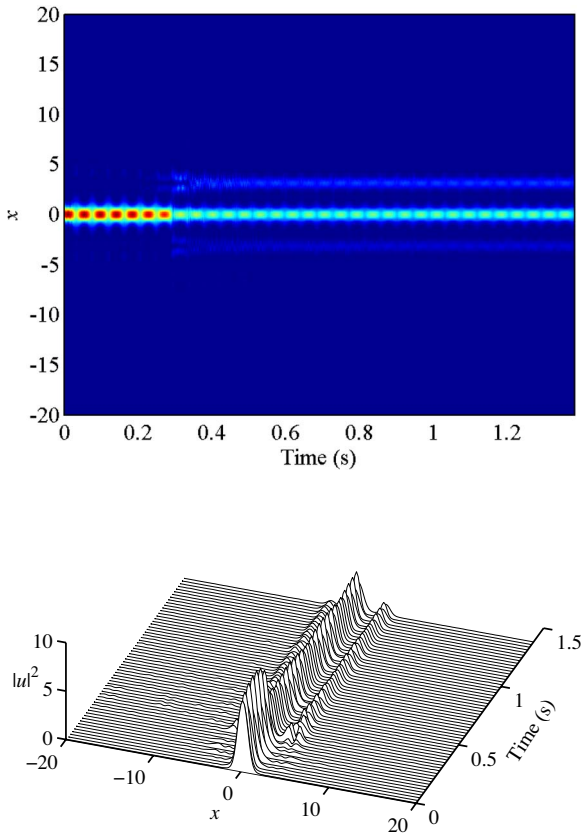

FIG. 8. (Color online) The same as in Figs. 6 and 7 for the fundamental soliton of type E in the second band gap, with initial norm $N=10.680$, under the action of the lattice management with $\varepsilon=1$ and $\omega=0.02$ (the initial shape of the soliton is the same as in panel E in the left column of Fig. 4). Emergence of side lobes in the soliton's profile is obvious.

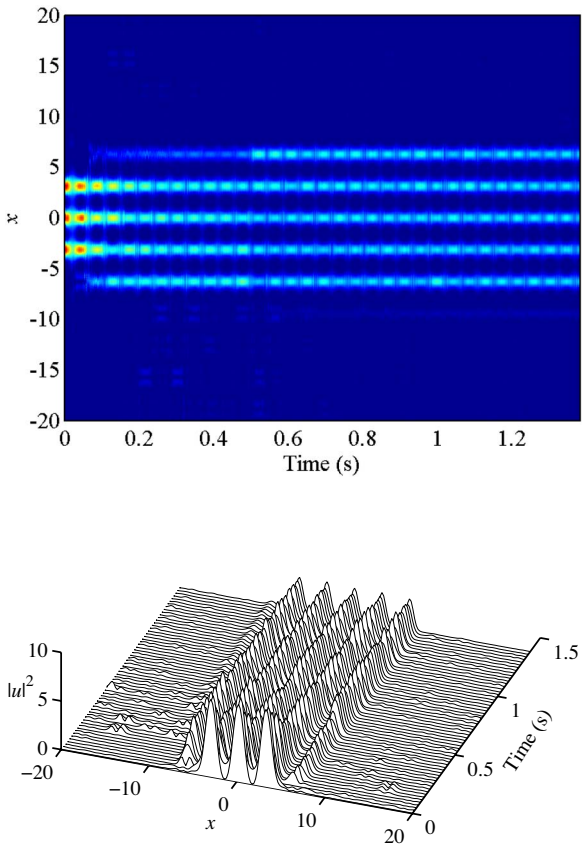

FIG. 9. (Color online) The same as in Fig. 8, but with the initial soliton of type G, shown in panel G in the right column of Fig. 3 (the norm of the initial soliton is $N=35.967$). Multiple formation of side lobes in the gap soliton under the action of the lattice management is observed in this case.

example of that is displayed in Fig. 10, for a compound of type J [cf. Fig. 5(c)]. If the spontaneous rearrangement of the subfundamental soliton into its fundamental counterpart is the only instability observed in the course of the evolution, the established soliton is classified as a stable one, as this rearrangement has nothing to do with the periodic modulation of the OL strength.

B. Stability diagrams

Data produced by massive simulations of Eq. (2), with initial conditions corresponding to various types of GSs in the first and second band gaps, are collected in the stability diagrams displayed in Fig. 11. The diagrams are drawn in the plane of the management parameters, viz., amplitude and frequency, ε and ω. The solitons are unstable to the right of the borders shown in Fig. 11. Each border appertains to a fixed value of N (see the figure), which is taken, for a given soliton species, very close to the right edge of the respective band gap, cf. Fig. 2 (i.e., this fixed N is, as a matter of fact, the largest norm available to the given branch of solitons). As said above, in the first band gap the unstable solitons suffer full destruction (see Fig. 7), while in the second band gap they develop the instability through the generation of sidelobes, see Figs. 8–10. It is noteworthy that, in either gap, the largest stability area is featured by the "lightest" species (one with the smallest value of N). In the first band gap, this is, naturally, the fundamental GS, of type A. In the second gap, it is, originally, the subfundamental soliton of type F, which is quickly transformed (with considerable loss of the norm), as explained above, by the intrinsic instability (unrelated to the lattice management) into a fundamental soliton which actually belongs to the fundamental branch, A, in the first band gap.

As said above, each stability border in Fig. 11 is drawn, as a matter of fact, for the largest value of N that can be attained by a given soliton species in the given band gap, as N is taken very close to the right edge of the band gap. A relevant issue is the change of the stability area [in the (ε,ω) plane] if smaller values of N are taken. A general result is that the direction of the change is *opposite* in the first and second band gaps: in the former one, the stability region monotonously shrinks with the decrease of N, while, in the second gap, the region occupied by solitons which are stable against the lattice management monotonously *expands* with decreasing N. These conclusions are valid for all species of the GSs in either band gap.

In a more particular form, the dependence of the stability area in the (ε,ω) plane on N is illustrated, in Fig. 12, by a set

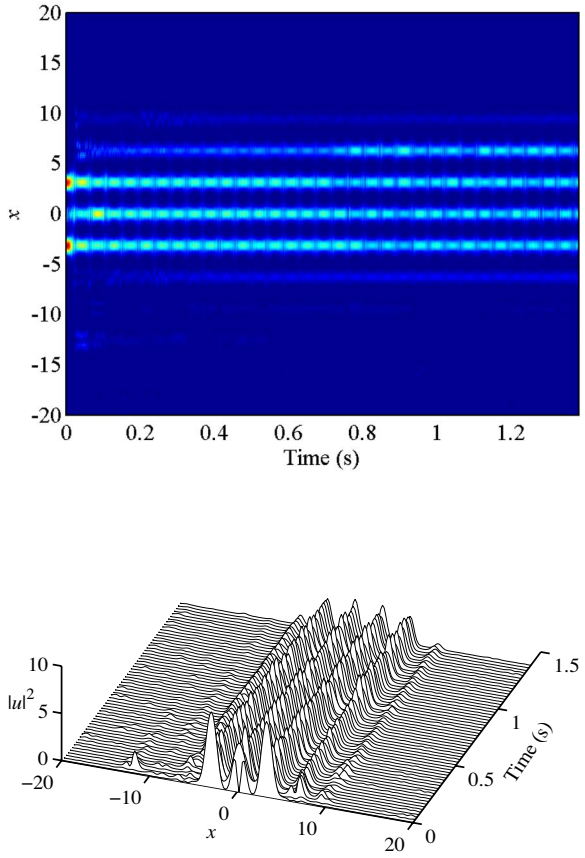

FIG. 10. (Color online) The same as in Figs. 8 and 9 but with the initial soliton of type J, shown in panel J in the right column of Fig. 3 (the norm of the initial soliton is $N=29.622$). In this case, as well as in the model with the static lattice, the subfundamental constituent of the compound quickly turns into a fundamental soliton; then, the formation of side lobes occurs, under the action of the lattice management. Spontaneous symmetry breaking is evident in this picture, as well as in Figs. 7–9.

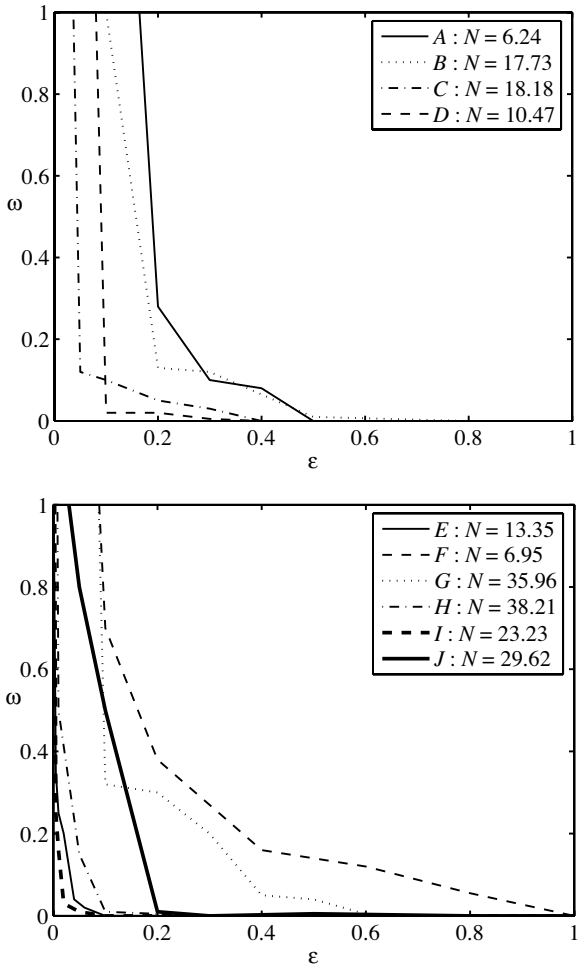

FIG. 11. Stability borders of various species of solitons in the first (top) and second (bottom) band gaps, in the plane of the lattice-management parameters, amplitude (ε) and frequency (ω), see Eq. (2). The species are identified by labels A through J as per Figs. 2–4. Each stability border is drawn at a fixed value of the soliton's norm indicated in the box. These values are chosen so as to take solitons of each type close to the right edge of the respective band gap.

of stability borders for the fundamental GSs, of types A and E, in both band gaps, drawn at different values of N. In both cases, the smallest and largest values of N are taken close to the left and right edges of the respective band gap (see Fig. 2), while intermediate values are chosen so as to adequately represent the situation in inner parts of the gaps.

A common feature of all stability charts displayed above is that the stability region is limited to $\varepsilon<1$, and in most cases, to $\varepsilon<0.5$. On the other hand, it is natural that the stability regions do not shrink to nil with the increase of the management frequency, as, in the case of a very high frequency, the ac (time-modulated) term in Eq. (2) averages to zero, and the remaining dc (constant) part readily supports GSs. The latter argument implies that the stability region may feature expansion with further increase of ω, provided that the management period, $2\pi/\omega$, becomes much smaller than a characteristic dispersion time of the solitons, which is ~ 0.5 (in the normalized units), as suggested by the soliton profiles displayed in Figs. 3 and 4. In other words, the expansion of the stability region may commence at $\omega \gtrsim 10$ (in physical units, this would correspond to the management frequency $\gtrsim 2\pi \times 10$ kHz), which is far larger than the range of values displayed in Figs. 11 and 12.

IV. CONCLUSIONS

The objective of this work was to investigate the stability of gap solitons (GSs) in the first two finite band gaps in the one-dimensional Gross-Pitaevskii equation (GPE) combining the repulsive nonlinearity and the periodic potential created by an optical lattice (OL), in the case when the lattice is subjected to the "management," in the form of the time-periodic modulation of its depth. The analysis, while performed in the normalized form, implied values of the modulation frequency (ω), stability/instability time, and OL depth, respectively, of roughly $2\pi \times 10$ Hz, 1.5 s, and 10 recoil energies, which are parameters relevant to the current experiments.

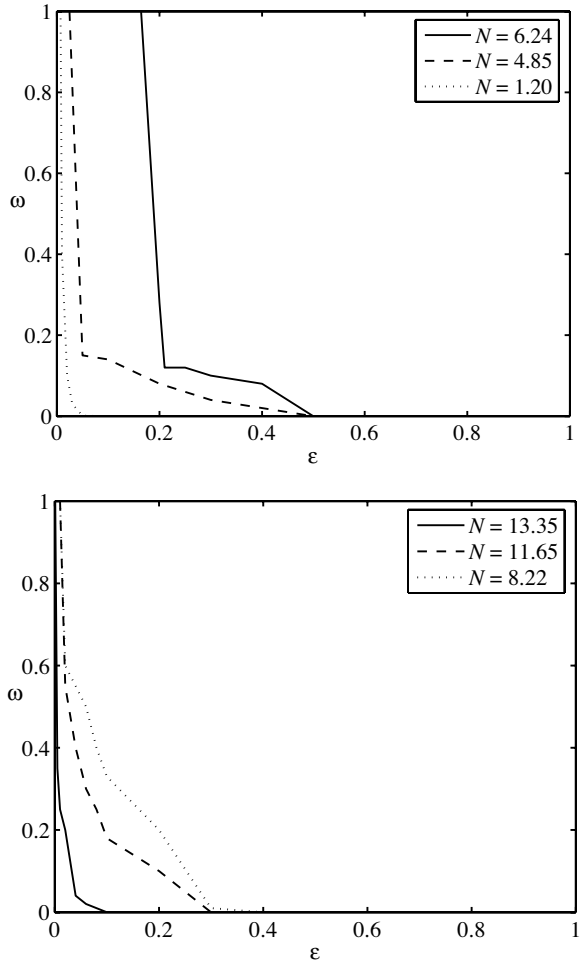

FIG. 12. Stability borders of the fundamental solitons, of types *A* and *E*, in the (ε,ω) plane, in the first (top) and second (bottom) band gaps, at different values of the fixed norm, *N*.

Before producing the results for the solitons under the lattice management, we have presented several GS species in the two band gaps, which include fundamental solitons, their bound states, and also the *subfundamental* soliton in the second band gap (along with complexes including subfundamental solitons), i.e., a localized structure featuring two peaks with opposite signs and zero between them, squeezed into a single well of the OL potential. This soliton is unstable (without any management), and quickly rearranges itself into a regular fundamental soliton, which is accompanied by the loss of up to half of its norm, and turns it into a fundamental soliton belonging to the first band gap (the same happens with subfundamental solitons which are constituents of various complexes). It is noteworthy too that, in the first band gap of the sufficiently strong OL, the bound state of two fundamental solitons (which is stable) is only possible when the solitons have opposite signs, and are separated by an empty potential well.

In the model with periodic time modulation of the OL depth, we have identified stability regions for various types of GSs in both band gaps, in the plane of ω and modulation amplitude (ε), at fixed values of the soliton's norm, *N*. In either band gap, the state with smallest *N* has the largest stability area (in the first and second gaps, these are, respectively, the fundamental soliton, and another fundamental one generated by the spontaneous transformation of the subfundamental soliton). However, a drastic difference between the two band gaps is that the stability area of each soliton species affected by the lattice management *increases* with *N* in the first gap, and *decreases* in the second one. Another difference between them is the outcome of the instability development: in the first band gap, unstable GSs are destroyed, while in the second one, they generate extra side lobes. In either case, the instability development features some spontaneous symmetry breaking.

Finally, it is worthy to note that extension of this work for two-dimensional solitons may be relevant to the theory and experiment alike. Results for this case will be reported elsewhere.

ACKNOWLEDGMENT

We appreciate valuable discussions with P. G. Kevrekidis. The work of B.A.M. was supported, in part, by the Israel Science Foundation through a Center-of-Excellence Grant No. 8006/03.

[1] O. Morsch and M. Oberthaler, Rev. Mod. Phys. **78**, 179 (2006).

[2] B. B. Baizakov, B. A. Malomed, and M. Salerno, Europhys. Lett. **63**, 642 (2003).

[3] N. K. Efremidis, J. Hudock, D. N. Christodoulides, J. W. Fleischer, O. Cohen, and M. Segev, Phys. Rev. Lett. **91**, 213906 (2003).

[4] J. Yang and Z. H. Musslimani, Opt. Lett. **28**, 2094 (2003); Z. H. Musslimani and J. Yang, J. Opt. Soc. Am. B **21**, 973 (2004).

[5] B. B. Baizakov, M. Salerno, and B. A. Malomed, in *Nonlinear Waves: Classical and Quantum Aspects*, edited by F. Kh. Abdullaev and V. V. Konotop (Kluwer Academic, Dordrecht, 2004), pp. 61–80; available online at http://rsphysse.anu.edu.au/~asd124/Baizakov_2004_61_NonlinearWaves.pdf.

[6] B. B. Baizakov, B. A. Malomed, and M. Salerno, Phys. Rev. A **70**, 053613 (2004).

[7] D. Mihalache, D. Mazilu, F. Lederer, Y. V. Kartashov, L.-C. Crasovan, and L. Torner, Phys. Rev. E **70**, 055603(R) (2004).

[8] Y. V. Kartashov, V. A. Vysloukh, and L. Torner, Phys. Rev. Lett. **93**, 093904 (2004).

[9] D. Mihalache, D. Mazilu, F. Lederer, B. A. Malomed, Y. V. Kartashov, L.-C. Crasovan, and L. Torner, Phys. Rev. Lett. **95**, 023902 (2005).

[10] C. J. Pethik and H. Smith, *Bose-Einstein Condensation in Di-*

lute Gases (Cambridge University Press, Cambridge, 2002).
[11] F. Kh. Abdullaev, B. B. Baizakov, S. A. Darmanyan, V. V. Konotop, and M. Salerno, Phys. Rev. A **64**, 043606 (2001); I. Carusotto, D. Embriaco, and G. C. La Rocca, *ibid.* **65**, 053611 (2002).
[12] B. B. Baizakov, V. V. Konotop, and M. Salerno, J. Phys. B **35**, 5105 (2002); E. A. Ostrovskaya and Yu. S. Kivshar, Phys. Rev. Lett. **90**, 160407 (2003).
[13] K. Winkler, G. Thalhammer, F. Lang, R. Grimm, J. H. Denschlag, A. J. Daley, A. Kantian, H. P. Büchler, and P. Zoller, Nature (London) **441**, 853 (2006).
[14] B. Eiermann, Th. Anker, M. Albiez, M. Taglieber, P. Treutlein, K.-P. Marzlin, and M. K. Oberthaler, Phys. Rev. Lett. **92**, 230401 (2004).
[15] Th. Anker, M. Albiez, R. Gati, S. Hunsmann, B. Eiermann, A. Trombettoni, and M. K. Oberthaler, Phys. Rev. Lett. **94**, 020403 (2005).
[16] T. J. Alexander, E. A. Ostrovskaya, and Y. S. Kivshar, Phys. Rev. Lett. **96**, 040401 (2005).
[17] P. G. Kevrekidis, B. A. Malomed, D. J. Frantzeskakis, A. R. Bishop, H. E. Nistazakis, and R. Carretero-Gonzalez, Math. Comput. Simul. **69**, 334 (2005).
[18] H. Sakaguchi and B. A. Malomed, J. Phys. B **37**, 2225 (2004).
[19] E. A. Ostrovskaya and Yu. S. Kivshar, Opt. Express **12**, 19 (2004); Phys. Rev. Lett. **93**, 160405 (2004).
[20] B. B. Baizakov, B. A. Malomed, and M. Salerno, Phys. Rev. A (unpublished).
[21] B. A. Malomed, *Soliton Management in Periodic Systems* (Springer, New York, 2006).
[22] J. J. García-Ripoll, V. M. Pérez-García, and P. Torres, Phys. Rev. Lett. **83**, 1715 (1999); J. J. G. Ripoll and V. M. Pérez-García, Phys. Rev. A **59**, 2220 (1999); F. Kh. Abdullaev and J. Garnier, *ibid.* **70**, 053604 (2004); F. Kh. Abdullaev, R. M. Galimzyanov, M. Brtka, and R. A. Kraenkel, J. Phys. B **37**, 3535 (2004).
[23] F. Kh. Abdullaev and R. Galimzyanov, J. Phys. B **36**, 1099 (2003); B. Baizakov, G. Filatrella, B. Malomed, and M. Salerno, Phys. Rev. E **71**, 036619 (2005).
[24] F. Kh. Abdullaev, J. G. Caputo, R. A. Kraenkel, and B. A. Malomed, Phys. Rev. A **67**, 013605 (2003); H. Saito and M. Ueda, Phys. Rev. Lett. **90**, 040403 (2003); G. D. Montesinos, V. M. Perez-Garcia, and P. J. Torres, Physica D **191**, 193 (2004); G. D. Montesinos, V. M. Perez-Garcia, and H. Michinel, Phys. Rev. Lett. **92**, 133901 (2004).
[25] M. Trippenbach, M. Matuszewski, and B. A. Malomed, Europhys. Lett. **70**, 8 (2005); M. Matuszewski, E. Infeld, B. A. Malomed, and M. Trippenbach, Phys. Rev. Lett. **95**, 050403 (2005).
[26] P. G. Kevrekidis, G. Theocharis, D. J. Frantzeskakis, and B. A. Malomed, Phys. Rev. Lett. **90**, 230401 (2003).
[27] A. Gubeskys, B. A. Malomed, and I. M. Merhasin, Stud. Appl. Math. **115**, 255 (2005).
[28] J. H. Denschlag, J. E. Simsarian, H. Häffner, C. McKenzie, A. Browaeys, D. Cho, K. Helmerson, S. L. Rolston, and W. D. Phillips, J. Phys. B **35**, 3095 (2002).
[29] L. Salasnich, A. Parola, and L. Reatto, J. Phys. B **39**, 2839 (2006).
[30] P. A. Clarkson, Proc. - R. Soc. Edinburgh, Sect. A: Math. **109**, 109 (1988); M. J. Ablowitz and P. A. Clarkson, *Solitons, Nonlinear Evolution Equations and Inverse Scattering* (Cambridge University Press, Cambridge, 1991).
[31] U. Dorner, P. Fedichev, D. Jaksch, M. Lewenstein, and P. Zoller, Phys. Rev. Lett. **91**, 073601 (2003); L. Fallani, L. De Sarlo, J. E. Lye, M. Modugno, R. Saers, C. Fort, and M. Inguscio, *ibid.* **93**, 140406 (2004).
[32] M. Krämer, L. Pitaevskii, and S. Stringari, Phys. Rev. Lett. **88**, 180404 (2002).
[33] Z. Rapti, P. G. Kevrekidis, A. Smerzi, and A. R. Bishop, J. Phys. B **37**, S257 (2004).
[34] P. G. Kevrekidis, D. J. Frantzeskakis, B. A. Malomed, A. R. Bishop, and I. G. Kevrekidis, New J. Phys. **5**, 64.1 (2003).
[35] S. Darmanyan, A. Kobyakov, and F. Lederer, JETP **86**, 682 (1998); P. G. Kevrekidis, A. R. Bishop, and K. Ø. Rasmussen, Phys. Rev. E **63**, 036603 (2001).
[36] T. Kapitula, P. G. Kevrekidis, and B. A. Malomed, Phys. Rev. E **63**, 036604 (2001).
[37] P. G. Kevrekidis (private communication).